Indian Journal of Chemical Technology
Vol. 24, May 2017, pp. 256-268

Experimental, surface characterization and computational evaluation of the acid corrosion inhibition of mild steel by methoxycarbonylmethyltriphenylphosphonium bromide (MCMTPPB)

Madhusudan Goyal, Ompal Yadav, Raman Kumar, Raj Kishore Sharma & Gurmeet Singh*

Department of Chemistry, University of Delhi, Delhi 110 007, India
E-mail: gurmeet123@yahoo.com

Received 9 April 2016; accepted 30 December 2016

The inhibition performance of the methoxycarbonylmethyltriphenylphosphonium bromide (MCMTPPB) on mild steel (MS) corrosion in 0.5 M H_2SO_4 has been evaluated using galvanostatic polarization (GP), potentiostatic polarization (PP), electrochemical impedance spectroscopy (EIS), scanning electron microscopy (SEM), and atomic force microscopy (AFM) techniques and complemented with the computational quantum calculations. GP study illustrates that the inhibition efficiency (%*IE*) increase with an increase in inhibitor concentration from 82.7% for 10^{-5} M to achieve 99.8% for 10^{-2} M. Polarization tafel curves clearly signify that MCMTPPB operates as a mixed type inhibitor. PP graph indicates that passivation was observed only for a lower concentration of MCMTPPB. Impedance results show that the double layer capacitance (C_{dl}) decrease and charge-transfer resistance (R_{ct}) increase with increase in the inhibitor concentration and hence increasing inhibition efficiency. Temperature influences the corrosion rate; inhibition efficiency and surface coverage decrease with increase in the temperature (298 K to 328 K). Surface characterization SEM with EDAX provide strong facts for the existence of inhibitor sheet over the MS surface. AFM studies are in good agreement with the results obtained by other techniques. Quantum chemical (QC) parameters obtained using AM1 Semi-empirical methods are found to be in good agreement with the experimentally measured inhibition efficiencies.

Keywords: MCMTPPB, Inhibitor concentration, MS, Polarization, EIS, SEM

The obviation of corrosion of metals and non-metals in diverse environments are of great importance in industries (chemical and electrochemical industries, food production, medical, nuclear, petroleum, and power) and also in daily life[1-3]. Among several methods of corrosion control, such as cathodic protection, anodic protection, coating and alloying etc., utilization of inhibitors is one of the most practical methods to ensure metal against acid corrosion due to its excellent mechanical and low cost[4-6]. The quality of a compound to serve as inhibitor is dependent on its ability to interact with π-orbital and/or nature of adsorption on metal surface, electrostatic attraction between the charged metal and charged inhibitor molecules, capable of forming bonds with the metal surface via electron transfer etc[7-10]. Organic additives containing heteroatoms such as phosphorus, sulfur, oxygen, nitrogen or those bearing multiple bonds, which are conceived as adsorption sites, are effective as corrosion inhibitors[11,12]. If they consist of a hydrocarbon part bonded to a polar or ionizable group also increase inhibition efficiency[13]. Phosphorous as a heteroatom in homologous series of organic additives is easily polarizable and has lower electronegativity as compared to other heteroatoms. Therefore, it is anticipated that phosphorous situated compounds should be more efficient in retarding the dissolution of metal in corrosive media[14-17].

Owing to the new environmental restrictions, searching for substitute compounds has led to the use of phosphonium ions, environmentally friendly compounds that have been effectively employed as inhibitors in corrosive systems. In this regard, quaternary phosphonium additives represent a promising preference for the design of "green" corrosion inhibitors. Moreover, low morbidity and biodegradability also satisfy the ever increasing requirements of the environmental regulation, which are recently imposed on the development of cleaner chemical inhibitors[18-21]. Hence, phosphonium additives are expected to act as potent corrosion inhibitors in corrosive media.

The aim of this work is to study the corrosion inhibition of MS in 0.5 M H_2SO_4 solution by

methoxycarbonylmethyltriphenylphosphonium bromide (MCMTPPB) as corrosion inhibitor using different techniques: weight loss; Galvanostatic; potentiostatic polarization; AC impedance studies and surface characterization (SEM & AFM) studies. The thermodynamic parameters were calculated and discussed. Quantum-chemical descriptors such as the energy of highest occupied molecular orbital ($E_{\_HOMO}$), the energy of lowest unoccupied molecular orbital (E_{LUMO}), the energy gap ($\Delta E = E_{LUMO} - E_{\_HOMO}$) were also computed and correlated with inhibition efficiency.

Experimental Section

Inhibitor compound

Methoxycarbonylmethyltriphenylphosphonium bromide (MCMTPPB) was obtained from Alfa alsar chemicals, Pro Lab marketing Limited, New Delhi, India. MCMTPPB solution of concentrations 10^{-2} M, 10^{-3} M, 10^{-4} M and 10^{-5} M were prepared in 0.5 M H_2SO_4 (analytical-grade chemical reagent) using distilled water. For each experiment, the freshly prepared solution was used. The structure of MCMTPPB is shown in Fig. 1.

Electrodes

Mild steel (MS) (Fe = 95.5%, C = 1.92%, Si = 0.15%, S = 0.15%, P = 0.17% and Mn = 0.60%) encapsulated in an epoxy resin (Araldite) with the exposed area of 1 cm^2 was used as the working electrode (WE). The surface of MS was abraded successively by emery papers of different grades, i.e. 150, 320, 400 and 600, and finely polished with 1000 and 1500 grades to obtain uniform mirror-like finishing. Further, MS was degreased with acetone and washed with distilled water. A platinum wire and dip type saturated calomel electrodes were used as counter and reference electrodes, respectively.

Weight loss measurements

Weight loss measurements were carried out by immersing MS coupons in a glass beaker containing 100 mL of corrosive media (0.5 M H_2SO_4) without and with different concentrations of inhibitor for an immersion time of 5 h. After the immersion time, the MS coupons were taken out, rinsed thoroughly with distilled water, dried and weighed accurately using digital balance (Accuracy: ± 0.1 mg, model No: AB – 54 S Mettler). The rectangular MS coupons with a dimension of (1 × 4 × 1) cm^3 were used in weight loss experiments. All experiments were carried out in static and aerated conditions. Each measurement was repeated for reproducibility and an average value was calculated.

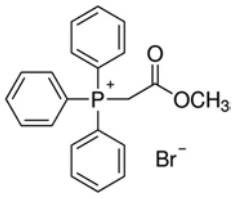

Fig. 1 — The molecular structure of methoxycarbonylmethyl triphenylphosphonium bromide (MCMTPPB)

Galvanostaticpolarisation(GP) studies

The galvanostatic polarisation (GP) studies were carried out in CHI 760C electrochemical workstation (CH Instruments, Austin, USA). The systems were studied using 0.5 M H_2SO_4 in the absence and presence of various concentrations of MCMTPPB. All measurements were conducted at 298 K, 308 K, 318 K and 328 K. The temperature was controlled thermostatically (±°C) and electrodes were introduced into the cell. The cell consisted of three electrodes, the working electrode (MS), a counter electrode (platinum), and a reference electrode (SCE). Before each electrochemical measurement, the working electrode was allowed to stand for 5 h in the test solution for the stabilization of open circuit potential (OCP). Each experiment was repeated three times and an average value was calculated. For Tafel measurements, the potential-current curves were recorded at a scan rate of 0.001 Vs^{-1} in the potential range of -0.9V to +0.0V. The corrosion parameters such as corrosion potential (E_{corr}), corrosion current (I_{corr}), cathodic Tafel slope (b_c), and anodic Tafel slope (b_a) were obtained from the Tafel extrapolation curves.

Potentiostatic polarisation (PP) studies

The electrode system used for this study was same as that used for GP studies. All measurements were performed at 298 K. Each system was allowed to attain OCP and then potential was given and the corresponding current was noted. The potential range was recorded in the range of 0.0V to +0.2V.

Electrochemical impedance spectroscopy (EIS)

EIS were carried out using AC signal with amplitude of 5 mV at OCP in the frequency range from 10^5 Hz to 1 Hz. The impedance parameters i.e. charge transfer resistance (R_{ct}) and frequency were obtained from Nyquist plots and doubled layer capacitance (C_{dl}) was calculated using the formula:

$$C_{dI} = \frac{1}{2_{\pi f_{max}} R_{Ct}} \quad \ldots (1)$$

where, f_{max} represents the frequency at which imaginary value reaches a maximum point on the Nyquist plot.

Temperature kinetic studies

The best correlation between the experimental results and isotherm functions was obtained using Langmuir adsorption isotherm. Thermodynamic adsorption parameters such as equilibrium constant for adsorption (K_{ads}), standard free energy change (ΔG°_{ads}), standard enthalpy change (ΔH°_{ads}) and standard entropy change (ΔS°_{ads}) were evaluated. The parameters were ensured with the spontaneity of the adsorption process and stability of the adsorbed layer on the MS surface.

Surface characterization methods

For surface analysis, polished MS specimens were immersed in 0.5 M H_2SO_4 without and with 10^{-2} M and 10^{-5} M of MCMTPPB for 24 h at room temperature. The SEM images (JEOL – JSM 6610) were obtained at the accelerating voltage of 20 kV at 1000× magnifications. EDX analysis was also carried out associated with SEM to identify the composition of the MS coupons in terms of weight percent. AFM measurements were performed using NAIO AFM nanosurf. The 3D images were recorded and analysed. The roughness of metal surface (RMS) was calculated using average area analysis.

Computational calculations

Quantum chemical calculations for MCMTPPB were carried out in the gas phase using Austin Model 1 (AM1) semi-empirical method. The Polak-Rieberre algorithm, which is very fast and accurate, was used for computational analysis. The geometry of the inhibitor molecule was optimized with energy parameters in the form of root mean square gradient at 0.1 kcal/Å mol and convergence limit of 0.1. The relation between the inhibition efficiency and quantum chemical calculation parameters, E_{HOMO}, E_{LUMO}, the energy gap ($\Delta E = E_{LUMO} - E_{\_HOMO}$), dipole moment, total negative charge on molecules, the fraction of electrons ($\Delta N_{inh \rightarrow M}$) transfer from inhibitor to MS and binding energy relationship were also investigated. These calculations were performed using Hyperchem 8.0 package program (Hypercube Inc., Florida, 2003).

Results and Discussion

Weight loss studies

From the weight loss study of MS coupons after 5 h immersion time in corrosive solutions (0.5 M H_2SO_4) in the absence and presence of different amounts of MCMTPPB, the inhibition efficiency and surface coverage were calculated and the results are given in Table 1.

The inhibition efficiency (% IE_W) and surface coverage (θ) of the inhibitor were obtained using equations (2) and (3):

$$\% \ IE_W = \frac{W_{corr\ (acid)} - W_{corr\ (inh)}}{W_{corr\ (acid)}} \times 100 \quad \ldots (2)$$

$$\theta = 1 - \left(\frac{W_{corr\ (inh)}}{W_{corr\ (acid)}} \right) \quad \ldots (3)$$

where $W_{Corr(inh)}$ and $W_{Corr(acid)}$ are the weight loss of the samples in the presence and absence of the inhibitor, respectively.

From the data in Table 1, the increase of % IE_W with inhibitor concentration primarily indicates that the magnitude of adsorption and surface coverage by inhibitor molecules on the surface of MS increases with inhibitor concentration[22].

Galvanostaticpolarisation (GP) studies

MethoxycarbonylmethylTriphenylPhosphonium Bromide (MCMTPPB) was performed as the inhibitor of corrosion of MS in 0.5 M H_2SO_4 acid at four concentrations viz., 1×10^{-2} M, 1×10^{-3} M, 1×10^{-4} M and 1×10^{-5} M. The effect of temperature on the corrosion inhibition of MS of MCMTPPB was studied by creating a three electrode assembly and maintaining them at four temperatures –298 K, 308 K, 318 K and 328 K. The experimental value of related electrochemical parameter such as corrosion potential (E_{corr}), cathodic and anodic Tafel slope values (b_c and b_a), corrosion current density (I_{corr}) and inhibition efficiencies (% IE) are given in Table 2 with representative Tafel polarization curves at 298 K shown in Fig. 2a.

Inhibition Efficiency (% IE) was calculated using the relationship:

Table 1 — The inhibition efficiency and surface coverage for MS in 0.5 M H_2SO_4 solution in presence of different concentrations from Weight Loss method

Solutions	Concentration (M)	Inhibition efficiency (% IE_W)	Surface coverage (θ)
H_2SO_4	0.5	-	-
MCMTPPB	10^{-2}	99.3	0.993
	10^{-3}	98.8	0.988
	10^{-4}	94.2	0.942
	10^{-5}	82.6	0.826

Table 2 — Corrosion parameters of MS in 0.5 M H_2SO_4 in the presence of MCMTPPB

Temp. (K)	Conc. (M)	$-E_{corr}$ (mV)	b_c (mV/dec)	b_a (mV/dec)	I_{corr} (mA/cm^2)	*IE* (%)	θ
298	10^{-2}	483	114.2	182.0	0.01619	99.81	0.9981
	10^{-3}	475	92.94	26.85	0.01416	99.83	0.9983
	10^{-4}	457	112.6	77.42	0.4629	94.74	0.9474
	10^{-5}	451	123.5	91.80	1.516	82.78	0.8278
	H_2SO_4	465	164.2	141.6	8.805	-	-
308	10^{-2}	513	110.4	242.8	0.05936	99.60	0.9960
	10^{-3}	493	104.5	135.9	0.05648	99.62	0.9962
	10^{-4}	462	118.0	76.82	1.350	90.99	0.9099
	10^{-5}	475	178.0	174.5	8.128	45.77	0.4577
	H_2SO_4	475	189.3	168.8	14.99	-	-
318	10^{-2}	507	115.3	207.2	0.03703	99.77	0.9977
	10^{-3}	502	104.2	128.1	0.0955	99.41	0.9941
	10^{-4}	473	169.7	179.8	7.184	56.16	0.5616
	10^{-5}	477	180.5	177.9	13.88	15.31	0.1531
	H_2SO_4	481	208.1	196.4	16.39	-	-
328	10^{-2}	499	131.4	159.8	0.4560	97.49	0.9749
	10^{-3}	520	117.4	94.76	0.6497	96.43	0.9643
	10^{-4}	461	166.8	169.8	12.63	30.72	0.3072
	10^{-5}	481	191.4	180.3	21.34	-17.06	-0.1706
	H_2SO_4	490	212.5	172.4	18.23	-	-

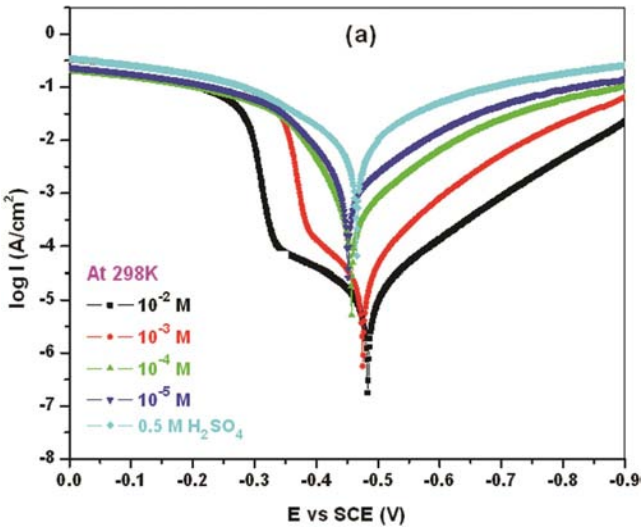

Fig. 2a — Representative Tafelpolarization curves for MS in 0.5 M H_2SO_4 containing different concentrations of MCMTPPB at temperatures 298K.

$$\%IE = \frac{I_{corr\,(acid)} - I_{corr\,(inh)}}{I_{corr\,(acid)}} \times 100 \quad \ldots (4)$$

where $I_{corr(acid)}$ and $I_{corr(inh)}$ symbolize the corrosion current density values nonappearance and appearance inhibitor, respectively. Corrosion current densities (I_{corr}) were extracted by Tafel extrapolating the cathodic and anodic lines to the corresponding corrosion potentials. From Table 2, it can be found that corrosion current density decreased with increase in the inhibitor concentration and %*IE* value improved. The inhibitor efficiency attained the maximum value of 99.8% at 10^{-2} M MCMTPPB. Surface coverage (θ) was calculated using the relationship:

$$\theta = 1 - \left(\frac{I_{corr\,(inh)}}{I_{corr\,(acid)}} \right) \quad \ldots (5)$$

Surface coverage data (Table 2) indicates that this additive was uniformly adsorbed over the metal surface but this decreased with a decrease in concentration of MCMTPPB. At a lower concentration (10^{-5} M), surface coverage dropped considerably because of the inability of MCMTPPB to block the active sites onto the metal surface. It can be clearly examined from Table 2 that the anodic Tafel slope (b_a) and the cathodic Tafel slope (b_c) values of MCMTPPB irregularly changed with inhibitor concentrations, indicating that MCMTPPB controlled both reactions. The inhibitory effect of MCMTPPB was not only due to adsorption alone but also due to mixed effects of blocking of active sites as well as the involvement of some other anions present in the solution[23].

There was no significant change in the OCP of inhibited solution from that of uninhibited solution (Fig. 2a). This was observed at all temperatures. This indicates that MCMTPPB was a mixed type of inhibitor and influenced both the cathodic and anodic partial processes to almost an equal extent[24].

Temperature influenced the corrosion rate in the presence of MCMTPPB (Table 2). Inhibition efficiency and surface coverage decreased with increase in temperature. At 10^{-2} M MCMTPPB inhibition efficiency reduced from 99.8% at 298 K to 97.2% at 328 K. The inhibition efficiencies are almost some trend at a higher temperature, which indicated that the adsorption of MCMTPPB was not merely a physical or a chemical adsorption but a comprehensive adsorption[25].

Potentiostatic polarization (PP) studies

Passivity affects the rates of corrosion process because it generates a protective/resistive layer that acts as a barrier to attack the surface of the metal by the environment[26]. Fig. 2b demonstrates the representative potentiostatic polarization curve for the corrosion of MS in 0.5 M H_2SO_4 solution and in the presence of various concentrations of MCMTPPB at 298 K. The anodic dissolution parameters such as critical current density (I_c), passivation potential (E_{pp}) and passive current (I_p) of MS in 0.5 M H_2SO_4 at various concentrations of inhibitor are depicted in Table 3. Critical current (I_c) was found to be decreased with increase in concentrations of MCMTPPB, which suggested that additive adsorbed on the metal surface. The passivation range was

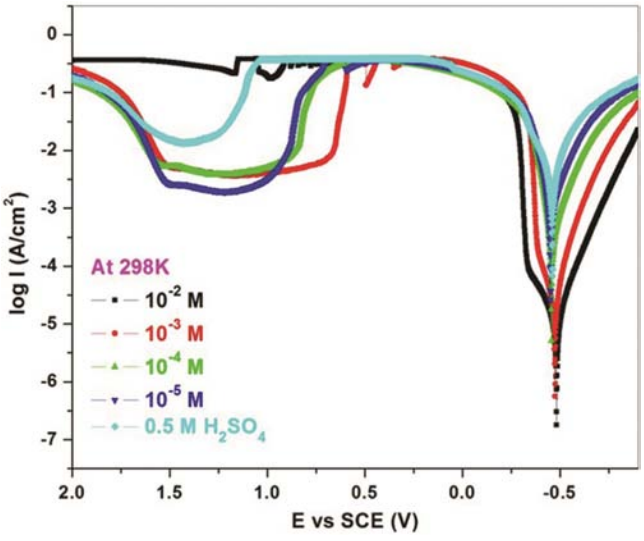

Fig. 2b — Potentiostatic polarisation curves for MS in 0.5 M H_2SO_4 containing different concentration of MCMTPPB at 298 K

666-1550 mV for various concentrations of the additive on metal surface, which was found to be larger and more covered than in the absence of additive[27].

At the lower concentration 10^{-5} M, the values of I_p were lower when compared with dissolution in the absence of additive as shown in Fig. 2b. These values showed that due to the synergistic effect of active assistance of bromide (Br^-) ions and other ions H_3O^+, HSO_4^-, SO_4^{2-} and OH^- present in the solution, MCMTPPB performed as a good passivator of MS in 0.5M H_2SO_4. The passivity might be due to the formation of additives of the type $(M–Inh)_{ads}$ / $(M–Inh–Br)_{ads}$/$(M–Inh–OH–Br)_{ads}$/$(M–Inh–Br–OH)_{ads}$/$(M-Br–OH–Inh)_{ads}$/ $(M–OH–Inh)_{ads}$ etc., which adsorb at the anodic sites to reduce the extent of corrosion. At higher concentration 10^{-2} M, MCMTPPB was not able to form a resistive/passive layer because of stearic hindrance. This might be due to the non-planar shape of inhibitor. Therefore, MCMTPPB did not passivate at higher concentrations but passivated well at lower concentrations.

Electrochemical impedance spectroscopy (EIS)

EIS studies for MS in 0.5 M H_2SO_4 without and with different concentrations of MCMTPPB were investigated at 298 K, which were presented as Nyquist and Bode plot in Fig. 3a and Fig.3b, respectively. The Nyquist plots of MS showed a single depressed semicircular loop and only one-time constant was observed in Bode diagrams. The depressed semi-circle is the characteristic of solid electrodes and is often referred to frequency dispersion which arises due to the roughness and other in homogeneities of the surface[28].The diameter of semicircle increased with the increase in concentrations of MCMTPPB. This diameter increase was more and more pronounced with increasing concentration of MCMTPPB, which indicated the adsorption of inhibitor molecules on the metal surface. The single capacitive loop expressed that the corrosion of MS in 0.5 M H_2SO_4 solution was mainly

Table 3 — Polarisation parameters for anodic dissolution of MS in 0.5 M H_2SO_4 in the presence of MCMTPPB

Solutions	Concentration (M)	I_c ($mAcm^{-2}$)	I_p ($mAcm^{-2}$)	E_{pp} mV(range)
H_2SO_4	0.5	376.0	35.1	1377-1552
MCMTPPB	10^{-2}	-	-	-
	10^{-3}	361.8	8.6	666-1532
	10^{-4}	374.8	10.3	874-1545
	10^{-5}	396.9	3.1	995-1525

controlled by a charge transfer process. In the evaluation of Nyquist plots, the difference in real impedance at lower and higher frequencies was considered as the charge transfer resistance (R_{ct}) and the double layer capacitance was calculated.

The inhibition efficiency of corrosion of MS was calculated from the eq. (6) using charge transfer resistance (R_{ct}):

$$IE\% = \frac{R_{ct} - R^{\circ}_{ct}}{R_{ct}} \times 100 \quad \ldots (6)$$

R^{o}_{ct} and R_{ct} are the charge transfer resistance values in the absence and presence of inhibitor, respectively.

The impedance data listed in Table 4 indicated that the charge transfer resistance (R_{ct}) values of inhibited compound increased with increase the concentration of MCMTPPB, which suggested the enhancement of adsorption of organic molecules (MCMTPPB) on the MS surface and blocking the steel surface efficiently. On the other hand, the values of double layer capacitance (C_{dl}) noticeably decreased with increase the concentration of MCMTPPB from 10^{-5} M to 10^{-2} M, which is most likely due to the decrease in local dielectric constant and/or increase in dimension of the electrical double layer, which suggested that the inhibitor molecule functioned by adsorption at the steel/solution interface[29]. The inhibition efficiencies calculated from EIS (Table 4), showed the same trend as those obtained from potentiodynamic polarization plot (Table 2) and weight loss measurement (Table 1).

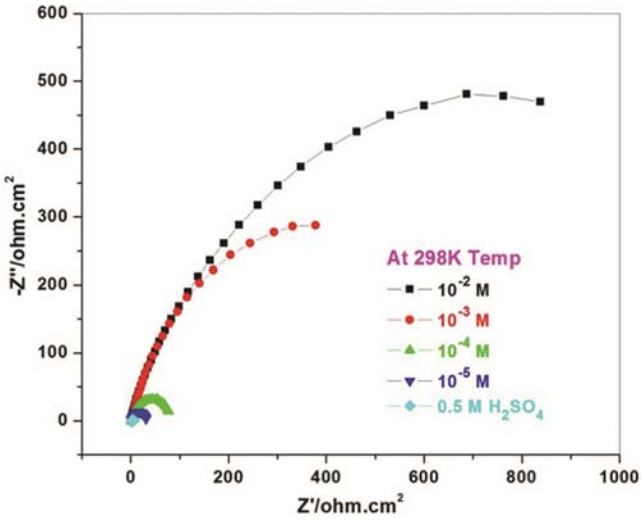

Fig. 3a — Nyquist plot for MS in 0.5 M H_2SO_4 and in the presence of various concentrations of MCMTPPB at 298 K

Adsorption isotherm and thermodynamically parameters

The inhibition efficiency (% *IE*) of molecules as good corrosion inhibitors mainly depends on their adsorption ability on the metal surface. The adsorption of inhibitors at the metal/solution is a substitution process which takes place through the replacement of water molecules by inhibitors molecules according to following process[30]:

$$Inh_{(sol)} + xH_2O_{(ads)} \leftrightarrow Inh_{(ads)} + xH_2O_{(sol)} \quad \ldots (7)$$

where $Inh_{(sol)}$ and $Inh_{(ads)}$ are inhibitor molecules in the solution and adsorbed on the metal surface, respectively. x is the number of water molecules replaced by molecules.

The surface coverage (θ) defined as *IE*/100, was tested by fitting to various adsorption isotherms like Langmuir (C/θ vs C), El-Awady (log $\frac{\theta}{C}$), Temkin (θ

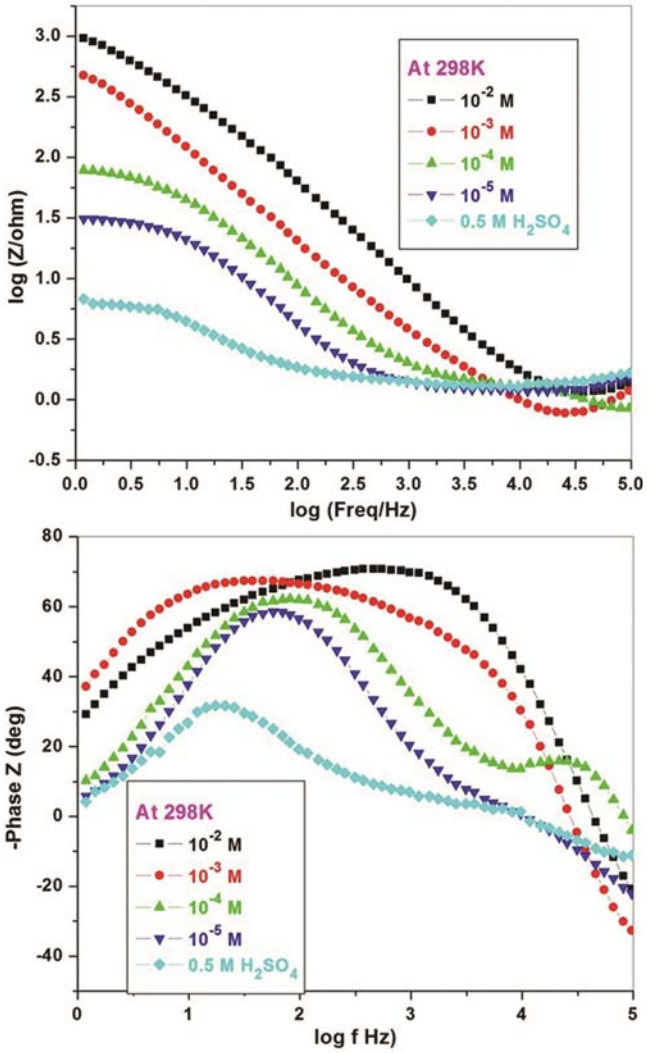

Fig. 3b — Bode plot for MS in 0.5 M H_2SO_4 and in the presence of various concentrations of MCMTPPB at 298 K

Vs log$\frac{\theta}{C}$), Freundlich (log θ Vs log C) and Flory–Huggins {log Vs log (1– θ)} with regression coefficient (R^2) 0.999, 0.876, 0.814, 0.803 and 0.998 respectively. The plot of C/θ versus C yields a straight line (Fig. 4) with R^2 close to 1, which suggests that the adsorption of inhibitor molecules follow Langmuir adsorption isotherm[31].However, the best fit was obtained with Langmuir isotherm which is presented graphically in Fig. 4.

According to Langmuir's isotherm, surface coverage is related to inhibitor concentration (C) by the following Equation (8):

$$\frac{C}{\theta}=\frac{1}{K_{ads}}+C \quad \ldots (8)$$

where K_{ads} is the equilibrium constant for adsorption process.

The K_{ads} values can be calculated from line intercept on C/θ axis and is associated to standard free energy change of adsorption (ΔG°_{ads}) as follows:

$$\Delta G^{\circ}_{ads}=-2.303RT\log(55.5K_{ads}) \quad \ldots (9)$$

where, R is universal gas constant (8.314 $Jmol^{-1}K^{-1}$), T denotes absolute temperature (K in kelvin) and value 55.5 is the concentration of water (in mol dm^{-3}) in the solution. Generally, the standard free energy of adsorption (ΔG°_{ads}) values of -20 $kJmol^{-1}$ or less negative are associated with an electrostatic interaction between charged molecules and charged metal surface then it is said that the inhibitor molecules are "physical adsorption" on the metal surface, whereas if the order is of -40 kJ mol^{-1} or more, involves charge sharing or transfer from the inhibitor to the metal surface to form a coordinate covalent bond then the inhibitor molecules are said to be "chemical adsorption". As can be seen from Table 5, In case of MCMTPPB, the values of ΔG°_{ads} range from –41.4 $kJmol^{-1}$ to –36.8 $kJmol^{-1}$, indicating that the adsorption of this inhibitor takes place through both chemical and physical adsorption namely mixed type with predominantly chemical one.

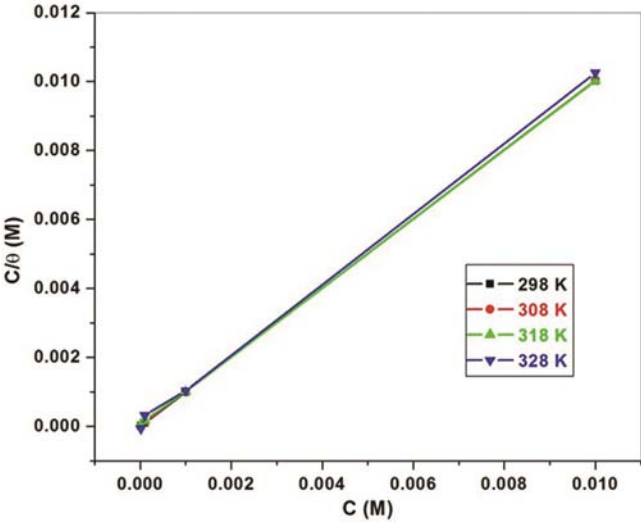

Fig. 4 — Representative Langmuir's adsorption isotherms for MS at different temperatures.

ΔG°_{ads} is related to change in enthalpy and entropy of adsorption, ΔH°_{ads} and ΔS°_{ads}, respectively, by following Equation (10):

$$\Delta G^{\circ}_{ads}=\Delta H^{\circ}_{ads}-T\Delta S^{\circ}_{ads} \quad \ldots (10)$$

The value of ΔH°_{ads} can be calculated by Van't Hoff Equation (11):

$$\ln K_{ads}=\frac{-\Delta H^{\circ}_{ads}}{RT}+\text{const.} \quad \ldots (11)$$

A plot of $\ln K_{ads}$ versus 1/T gives a straight line and ΔH°_{ads} values calculated from the slope of the straight line (slope = ΔH°_{ads} /R) drawn from the data given in Table 5. The negative value of enthalpy (ΔH°_{ads}) behaviour can be interpreted on the basis that at a higher temperature more desorption of the adsorbed inhibitor molecules occurred from the MS surface. The standard entropy of inhibitor adsorption, ΔS°_{ads}, were calculated from Eq. (10) and recorded in Table 5. As expected, the values of ΔS°_{ads} were negative, because exothermic adsorption process was found to be associated with a decrease in entropy. Orderliness increased as inhibitor molecules adsorbed on the metal surface, resulting in a decrease in entropy[32].

Table 4 — EIS Data for MS in 0.5 M H_2SO_4 in the absence and presence of different concentrations of inhibitor MCMTPPB

Solutions	Concentration (M)	R_{ct} (Ω cm^2)	C_{dl} (μF cm^{-2})	f_{max}	IE (%)
H_2SO_4	0.5	4.954	15935	2.017	-
MCMTPPB	10^{-2}	1481.17	0.2223	483.6	99.66
	10^{-3}	746.867	0.7413	287.3	99.33
	10^{-4}	85.514	57.105	32.61	94.20
	10^{-5}	31.173	388.45	13.15	84.11

Table 5 — Adsorption parameters at different temperatures studied for MCMTPPB

Temperature (K)	K_{ads} x 10^4 M^{-1}	$-\Delta G^{\circ}_{ads}$ (kJ mol^{-1})	$-\Delta H^{\circ}_{ads}$ (kJ mol^{-1})	$-\Delta S^{\circ}_{ads}$ (JK^{-1} mol^{-1})
298	33.33	41.465		163.28
308	12.50	40.345	90.123	161.61
318	2.00	36.808		167.65
328	1.66	37.468		160.53

Effect of temperature and activation energy

The effect of temperature on the performance of the inhibitors for MS in 0.5 M H_2SO_4 solutions in the absence and presence of various concentrations of MCMTPPB inhibitor at different temperatures (298 K to 328 K) was studied by using potentiodynamic polarization technique. The corrosion parameters and inhibition efficiencies are given in Table 2. This data indicated that corrosion current increased and inhibition efficiencies decreased with increasing temperature. At 10^{-2} M MCMTPPB, inhibition efficiency reduced from 99.8% at 298 K to 97.4% at 328 K. Adsorption became weaker at very high temperatures, thereby leading to lower adsorption resulting in increased corrosion rates.

Table 6 — Activation parameters for the corrosion of MS in the absence and presence of MCMTPPB

Concentration (M)	E_{act} (kJ mol^{-1})
0.5 M H_2SO_4	8.1916
10^{-2}	33.930
10^{-3}	42.875
10^{-4}	41.601
10^{-5}	30.488

Arrhenius proposed a relation to evaluate the effect of temperature on the rate of corrosion as follows[33]:

$$\mathrm{Log}\, i_{corr} = \mathrm{Log}\, A - \left(\frac{E_{act}}{RT}\right) \quad \ldots (12)$$

where A is the Arrhenius pre-exponential constant. The values of E_{act} (Table 6) were calculated from the plots of Log (i_{corr}) vs. 1/T. It was observed from Table 6 that the E_{act} values were reported between 30.4 to 42.8 $kJmol^{-1}$ for concentrations of MCMTPPB. The value of E_{act} in the presence of MCMTPPB was high in comparison with its absence, which indicated a strong inhibitive action of MCMTPPB by increasing the energy barrier for the corrosion process. Thus, activation energy values supported that MCMTPPB inhibitor was chemically adsorbed on the MS surface.

Scanning electron microscope (SEM)

To establish the interaction of inhibitor molecule with the metal surface, SEM images were taken. The SEM images of MS in 0.5 M H_2SO_4 solution in the absence and presence of 10^{-2} M and 10^{-5} M MCMTPPB after 24 h exposure at the 1000x magnification are given in Fig. 5 (b-d), respectively.

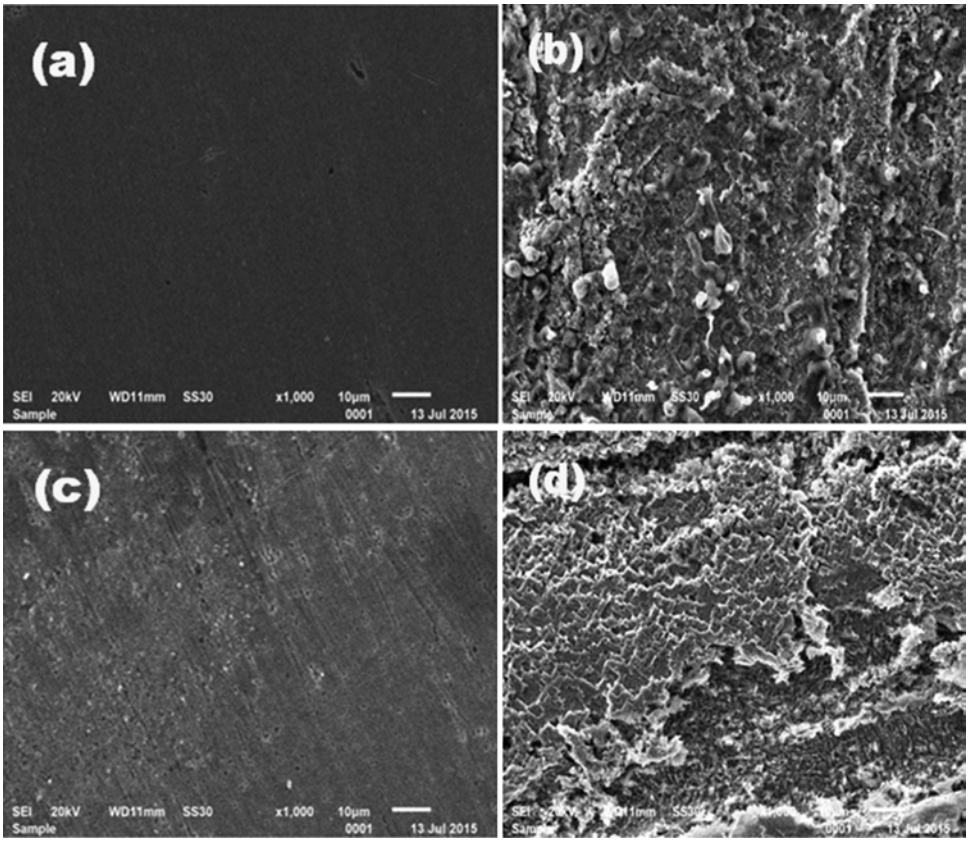

Fig. 5 — SEM images of (a) Plain MS surface; (b) MS in 0.5 M H_2SO_4; (c) MS in 0.5 M H_2SO_4 + 10^{-2} M MCMTPPB and (d) MS in 0.5 M H_2SO_4 + 10^{-5} M MCMTPPB, after 24 h exposure at the x1000 magnification.

Fig. 5(a) shows that the plain surface of the metal is absolutely free from any pits and cracks with a uniform modification of the MS surface. The photomicrograph of MS in the absence of inhibitor showed some cracks and pits due to the attack of corrosive solution, while in the presence of inhibitor, it can be seen from Fig. 5 (c and d) that the dissolution rate of MS considerably reduced and the smooth surface appeared by formation of a protective layer on the metal surface. The experimental results showed that the effectiveness of the MCMTPPB as a corrosion inhibitor formed an absorbing layer on MS surface, which inhibited corrosion[34,35].

Energy dispersive X-ray spectroscopy (EDXS)

The composition of the film precipitated on the MS surface was studied by EDXS analysis. The test was done on the surface of the steel immersed in the solutions with MCMTPPB at 24 h immersion times. The results of EDXS analysis are shown in Fig. 6 and data given in Table 7.

Fig. 6 shows typical EDXS spectra of the samples, where the peak position and intensity give information about the identity and the amount of atoms, respectively. Data from Table 7 reveals that the film precipitated on the MS surface immersed in the solution with MCMTPPB molecule was composed of *P*, *O*, *Br* and *Fe* elements[36,37]. This clearly indicates that the ions released by the MCMTPPB would have formed the protective film over the MS surface.

Table 7 — EDXS Data for MS in 0.5 M H_2SO_4 in the absence and presence of different concentrations of inhibitor MCMTPPB

Solutions	*Fe*	*O*	*S*	*P*	*Si*	*Br*
0.5M H_2SO_4	81.6	13.6	0.67	0.13	0.15	-
Plain Mild Surface	95.5	1.47	0.15	0.17	0.15	-
10^{-2}M MCMTPPB	91.8	4.07	0.42	0.17	-	0.47
10^{-5}M MCMTPPB	92.4	5.33	0.26	0.10	-	0.12

Atomic force microscopy (AFM)

AFM is a powerful technique to investigate the surface morphology studies which has been recently used to study the influence of inhibitors on the metal/corrosive solution interface[38]. The three-dimensional (3D) images of AFM were recorded and analyzed. Fig.7 (a) showed the AFM images of a plain surface of MS.This micrograph showed that the plain steel surface is free from any sort of impurity and pit. There is almost no roughness at all on the surface.

AFM image of MS surface after exposure to 0.5 M H_2SO_4 solution, shown in Fig.7 (b), the surface of MS electrode exposed to corrosive solution had a considerably porous structure with large and deep pores. The roughness of surface was 668.1 nm.

Figure7 (c, d) clearly indicates that the surface is smoother in the presence of 10^{-2} M and 10^{-5} M MCMTPPB, which suggest the adsorption of inhibitor molecule on MS surface and reduction in the corrosion rate. The surface roughness of MS after the addition of 10^{-2} M and 10^{-5} M MCMTPPB were 138.3

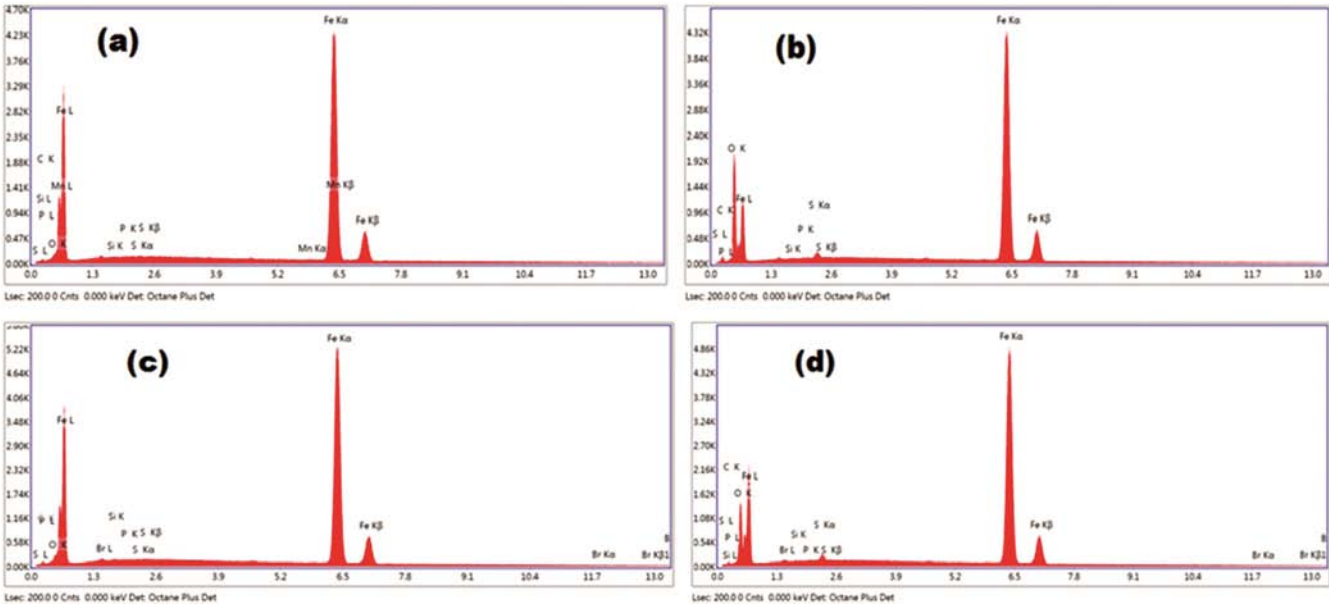

Fig. 6 — EDX spectra of (a) Plain MS surface; (b) MS in 0.5 M H_2SO_4; (c) MS in 0.5 M H_2SO_4 + 10^{-2} M MCMTPPB and (d) MS in 0.5 M H_2SO_4 + 10^{-5} M MCMTPPB.

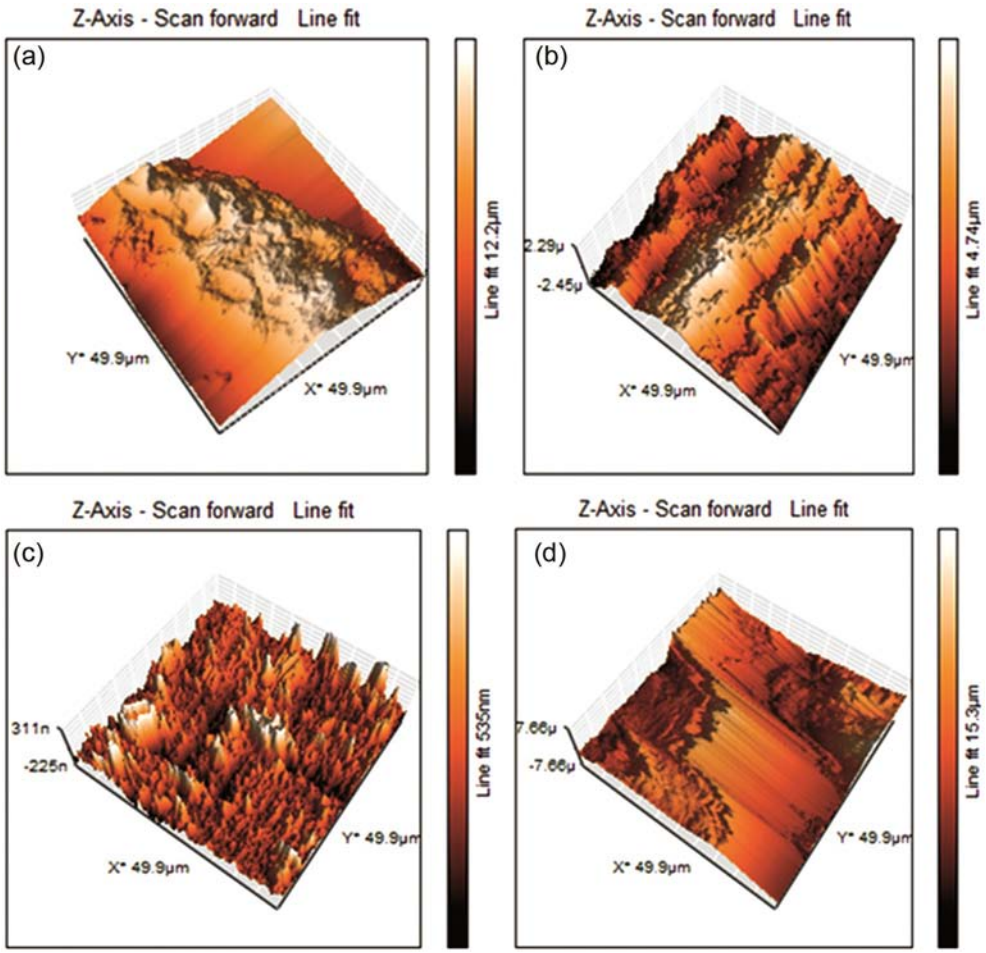

Fig. 7 — AFM images of (a) abraded MS surface; (b) MS in 0.5 M H_2SO_4; (c) MS in 0.5 M H_2SO_4 + 10^{-2} M MCMTPPB and (d) MS in 0.5 M H_2SO_4 + 10^{-5} M MCMTPPB

and 165.4 nm, respectively. The inhibitor molecule MCMTPPB adsorbed on the MS surface and protected the metal against corrosion.

Quantum chemical (QC) calculation

The computed quantum chemical parameters such as the energy of highest occupied molecular orbital (E_{HOMO}), the energy of lowest unoccupied molecular orbital (E_{LUMO}), LUMO-HOMO energy gap ($\Delta E_{L\text{-}H}$), dipole moment (μ), binding energy and heat of formation etc. are summarized in Table 8. The optimized structure, Mulliken charges and frontier orbital energy distribution of HOMO and LUMO of MCMTPPB are given in Fig. 8. The HOMO and LUMO energies are correlated with percent inhibition efficiencies.

Frontier orbital theory is useful in predicting adsorption centers of the inhibitor molecule responsible for the interaction with surface metal atoms. I.B. Obot *et al.*[39] suggested that when a molecule had similar frontier orbitals, its inhibition efficiency could be correlated to the energy levels of HOMO and LUMO and the difference between them. It has been well documented in the literature that higher the value of E_{HOMO}, greater is the ease for an inhibitor to donate electrons to unoccupied d orbital of metal atom and higher is the inhibition efficiency. Further, lower the E_{LUMO}, easier is the acceptance of electrons from metal atom to form feedback bonds.

Table 8 — Quantum chemical parameters of MCMTPPB using AM_1 semi-empirical method, Hyper Chem 8.0

Total energy (kcal mol^{-1})	-94174.17
Energy of HOMO (eV)	-7.84102
Energy of LUMO (eV)	-0.53019
Energy gap ($\Delta E_{L\text{-}H}$)	7.31083
Binding energy (kcal mol^{-1})	-4836.44
Heat of formation (kcal mol^{-1})	15.71
Dipole moment(Debye)	4.783
Molecular point group	C_1
Number of transfer electron ($\Delta N_{Inh\rightarrow M}$)	0.3849

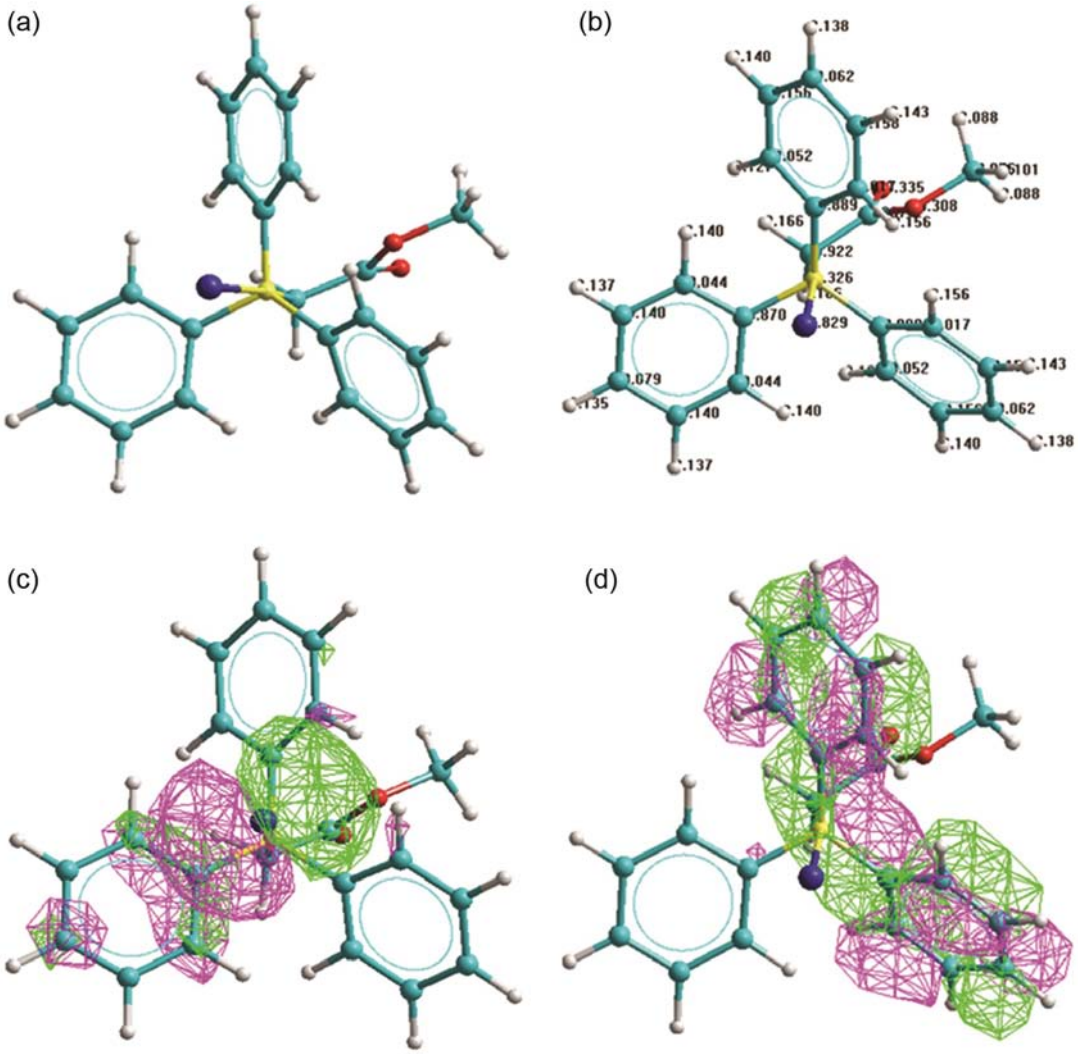

Fig. 8 — Computed quantum parameters for MCMTPPB: (a) Ball and Stick optimized structure; (b) Mulliken charges; (c) HOMO frontier orbital energy distribution, and (d) LUMO frontier orbital energy distribution.

The gap between LUMO – HOMO energy levels of molecules was another important parameter that needs to be considered. Smaller the value of $\Delta E_{L\text{-}H}$ of an inhibitor, higher is the inhibition efficiency of that inhibitor.

The negative binding energy (Table 8) indicated that methoxycarbonylmethyltriphenylphosphonium ion was very stable and was less prone to be split or broken apart. Molecular point group C_1 suggested that MCMTPPB was anon-planar molecule with no symmetry elements. Therefore, the coverage of the surface was not as uniform as observed for planar molecules. A Large value of dipole moment suggested that it was a polar compound and could easily donate π-electrons forming strong dπ–pπ bonding. Analysis of Mulliken population to probe the adsorption centers presence in an inhibitor molecule has been widely reported. Several researchers are of the opinion that, higher the magnitude of negative charge on hetero or any atom and higher the number of such atoms, the more strongly it can be adsorbed on the metal surface. In the Fig 8 (b), the negative charge on the oxygen atom, phosphorous atom, carbon of the three phenyl rings attached to the central P atom and CH_2 carbon compared to other carbon atoms in the molecule, connected to the donating electrons, were relevant to the inhibition efficiency. This suggested that these process could be possible in centers of adsorption[40,41].

The number of transferred electrons ($\Delta N_{inh\rightarrow M}$) was also calculated depending on the quantum chemical method[42,43]:

$$\Delta N_{inh\text{-}M} = \frac{X_{Fe} - X_{inh}}{2(\eta_{Fe} + \eta_{inh})} \quad \ldots (13)$$

where χ_{Fe} and χ_{inh} denote the absolute electro negativity of iron and the inhibitor molecule, respectively; η_{Fe} and η_{inh} denote the absolute hardness of iron and the inhibitor molecule, respectively. These quantities are related to electron affinity (A) and ionization potential (I)

$$\chi = (I+A)/2 \quad \ldots (14)$$

$$\eta = (I-A)/2 \quad \ldots (15)$$

I and A are related in turn to E_{HOMO} and E_{LUMO}

$$I = -E_{HOMO} \quad \ldots (16)$$

$$A = -E_{LUMO} \quad \ldots (17)$$

Values of χ and η were calculated using the values of I and A, obtained from quantum chemical calculation. Using a theoretical χ value of 7eV/mol and η value of 0eV/molfor iron atom, $\Delta N_{Inh \rightarrow M}$, the fraction of electrons transferred from inhibitor to the iron molecule was calculated. Values of $\Delta N_{Inh \rightarrow M}$ showed inhibition effect resulted from electrons donation. In this study, the MCMTPPB was the donator of electrons while the MS surface was the acceptor. The inhibition efficiency increased with increasing electron-donating ability at the metal surface. The compound MCMTPPB was bound to the metal surface and thus formed inhibition adsorption layer against corrosion.

Conclusion

From the overall data of adsorption of MCMTPPB on MS surface in acid solution studied with the help of galvanostatic, potentiostatic polarisation and electrochemical impedance and confirmed by surface characterization and quantum chemical studies, it can be concluded that

i. Galvanostatic polarisation measurement show that MCMTPPB is a mixed type of inhibitor as is evident from the insignificant shift of OCP values. The inhibition efficiency and surface coverage increases with increase in concentrations of inhibitor.

ii. Adsorption of the inhibitor is found to follow the Langmuir's isotherm. Thermodynamic adsorption parameters such as K_{ads}, ΔG°_{ads}, ΔH°_{ads}, and ΔS°_{ads}, show that the MCMTPPB inhibitor molecule adsorbed on the MS surface by a spontaneous exothermic process.

iii. Potentiostatic polarisation measurement indicate that this inhibitor MCMTPPB passivated the metal at lower concentrations.

iv. Impedance measurements show that the double-layer capacitance decreased and charge-transfer resistance increases with increase in the inhibitor concentrations and hence increases in inhibition efficiency.

v. The surface morphology as studied by SEM-EDX S and AFM supplement, the electrochemical results according to which the extent of corrosion is reduced to a large extent in the presence of inhibitor MCMTPPB than in its absence.

vi. Quantum chemical (QC) calculations show that the inhibitor molecules also acted as an electron acceptor when they interacted with the MS surface confirming that adsorption of MCMTPPB on the MS surface is a comprehensive one.

vii. The %*IE* obtained from weight loss, polarisation and AC impedance are in reasonably good agreement.

viii. The experimental results are supported by the theoretical data also.

References

1 Vashisht H, Bahadur I, Kumar S, Goyal M S, Kour G, Singh G, KataraSeru L & Ebenso E E, *J Mol Liq*, 224 (2016) 19.

2 Maruthamuthu S, Mohanan S & Rajasekar A, *Indian J Chem Technol*, 12 (2005) 567.

3 Tiu B D B & Advincula R C, *React Funct Polym*, 95 (2015) 25.

4 Carmona J, Garcés P & Climent M A,*Corros Sci*, 96 (2015) 102.

5 Asemani H R, Ahmadi P, Sarabi A A & Mohammadloo H E, *Prog Org Coatings*, 94 (2016) 18.

6 Arthanareeswari M, Sankara Narayanan T S N, Kamaraj P & Tamilselvi M, *Indian J Chem Technol*, 17 (2010) 167.

7 Kumar S, Vashisht H, Olasunkanmi L O, Bahadur I, Verma H, Singh G, Obot I B & Ebenso E E, *Sci Rep*, 6 (2016) 30937.

8 Bhrara K & Singh G, *Corros Eng Sci Technol*, 42 (2007) 137.

9 Theory S A H & Walters F H, *J Chem Educ*, 68 (1991) 29.

10 Sharma M, Chawla J & Singh G, *Indian J Chem Technol*, 16 (2009) 339.

11 Niass S O, Touhami M E B N, Hajjaji N, Srhiri A & Takenouti H, *J Appl Electrochem*, 31 (2001) 85.

12 Danaee I, Moallem Z, Eskandari H & Nikmanesh S, *Indian J Chem Technol*, 23 (2016) 345.

13 Jangu C & Long T E, *Polym (United Kingdom)*, 55 (2014) 3298.

14 Morad M S, *et al, Corros Sci*, 42 (2000) 1307.

15 Wang M L, Liu B L & Lin S J, *J Chinese Inst Chem Eng*, 38 (2007) 451.

16 Walia M & Singh G, *Surf Eng*, 21 (2005) 176.
17 Hosseini S M A, Quanbari M & Salari M, *Indian J Chem Technol*, 14 (2007) 376.
18 Tsunashima K, Kawabata A & Matsumiya M, *Electrochem commun*,13 (2011) 178.
19 Atefi F, Garcia M T, Singer R D & Scammells P J, *Green Chem*, 11 (2009) 1595.
20 Taw S M & Negm N A, *J Mol Liq*, 215 (2016) 185.
21 Xue Y, Xiao H & Zhang Y, *Int J Mol Sci*, 16 (2015) 3626.
22 Wang X, Yang H & Wang F, *Corros Sci*, 53 (2011) 113.
23 Bhrara K & Singh G, *Appl Surf Sci*, 253 (2006) 846.
24 Wahdan M H, Hermas A A & Morad M S, *Mater Chem Phys*, 76 (2002) 111.
25 Ahamad I, Prasad R & Quraishi M A, *Corros Sci*, 52 (2010) 933.
26 Sekunowo O I, Adeosun S O & Lawal G I, *Int J Sci Tech*, 2 (2013) 139.
27 Singh M R, Bhrara K & Singh G, *Portugaliae Electrochimica Acta*, 26 (2008) 479.
28 Yadav D K, Maiti B & Quraishi M A, *Corros Sci*, 52 (2010) 3586.
29 Chaitra T K, Mohana K N S & Tandon H C, *J Mol Liq*, 211 (2015) 1026.
30 Scendo M & Trela J, *Int J Electrochem Sci*, 8 (2013) 8329.
31 Abdallah M, Defrawy A M E l, Zaafarany I A, Sobhi M & Elwahy A H M, *Int J Electrochem Sci*, 9 (2014) 2186.
32 Nataraja S E, Venkatesha T V & Tandon H C, *Corros Sci*, 60 (2012) 214.
33 Bhrara K, Kim H & Singh G, *Corros Sci*, 50 (2008) 2747.
34 Saranya J, Sowmiya M, Sounthari P, Parameswari K, Chitra S & Senthilkumar K, *J Mol Liq*, 216 (2016) 42.
35 El-lateef H M A, Abu-dief A M & El-gendy B E M, *J Electroanalytical Chem*, 758 (2015) 135.
36 Prabhu D, *et al*, *Int J Chem Tech Res*, 5 (2013) 2690.
37 Yadav M, Kumar S, Sinha R R, Bahadur I & Ebenso E E, *J Mol Liq*, 211 (2015) 135.
38 Mourya P, Singh P, Rastogi R B & Singh M M, *Appl Surf Sci*, 380 (2016) 1.
39 Obot I B, Obi-Egbedi N O & Umoren S A, *Corros Sci*, 51 (2009) 276.
40 Gece G & Bilgiç S, *Corros Sci*, 51 (2009) 1876.
41 Arslan T, Kandemirli F, Ebenso E E, Love I & Alemu H, *Corros Sci*, 51 (2009) 35.
42 John S & Joseph A, *Int J Chem Technol*, 19 (2012) 195.
43 Olasunkanmi L O, Kabanda M M & Ebenso E E, *Phys E Low-Dimens Syst Nanostruct*, 76 (2016) 109.